Liu *et al.*
European Journal of Medical Research (2025) 30:373
https://doi.org/10.1186/s40001-025-02541-3

European Journal of Medical Research

RESEARCH

Open Access

The potential of *MCM8* as a biomarker in esophageal carcinoma: a comprehensive analysis integrating m6a methylation and angiogenesis

Xu-Sheng Liu[2,3†], Yong Xu[4†], Li-Song Dai[5†], Ao Li[6], Jie Liu[7], Yu Zhang[2], Jin Xie[8*] and Zhi-Jun Pei[1*]

Abstract

Background Effective biomarkers for esophageal carcinoma (ESCA) are currently lacking. Here, we examined the role of minichromosome maintenance complex component 8 (MCM8) as a diagnostic and prognostic marker in ESCA and its association with m6a methylation and angiogenesis, and constructed a competing endogenous RNA (ceRNA) network.

Methods Clinical data and gene expression profiles were obtained from The Cancer Genome Atlas and Gene Expression Omnibus datasets. Differential gene expression analysis was performed using DESeq2 and limma packages. The prognostic significance of MCM8 expression regarding overall survival (OS) was examined using the Cox proportional hazards model. Receiver Operating Characteristic (ROC) analysis was used to assess the diagnostic potential of MCM8. MCM8 expression in ESCA tissues was evaluated by immunohistochemical staining on a tissue microarray. Pearson correlation analysis identified co-expressed genes, followed by Gene Ontology and Kyoto Encyclopedia of Genes and Genomes pathway enrichment analyses. The GEPIA online tool was used to examine the relationship between MCM8 and m6a methylation as well as angiogenesis-related genes. MicroRNA and long noncoding RNA predictions were made using miRWalk, MicroT-CDS, ENCORI, and miRNet tools to construct the ceRNA network.

Results MCM8 was significantly overexpressed in tumor tissues and showed high diagnostic accuracy in the ROC analysis with an area under the curve of 0.920. Kaplan–Meier survival analysis revealed that high MCM8 expression correlated with poorer OS and disease-specific survival. Pearson correlation analysis identified a significant correlation between MCM8 and several m6a methylation-related genes such as HNRNPA2B1 and YTHDF1, as well as PTK2, an angiogenesis-related gene. A ceRNA network including MCM8, PURPL/hsa-miR- 135a- 5p/MCM8 was successfully predicted and constructed.

Conclusions MCM8 is a promising biomarker in ESCA and it is associated with m6a methylation and angiogenesis, showing potential as a therapeutic target. The ceRNA network provided insight into the pathogenesis of ESCA.

Keywords *MCM8*, Esophageal carcinoma, m6a, Angiogenesis, ceRNA

†Xu-Sheng Liu, Yong Xu and Li-Song Dai have contributed equally.

*Correspondence:
Jin Xie
153162220@qq.com
Zhi-Jun Pei
zjpei@suda.edu.cn
Full list of author information is available at the end of the article

Introduction

Esophageal carcinoma (ESCA) is a significant global health concern due to its high incidence and mortality rates. It is the seventh most common cancer worldwide and the sixth leading cause of cancer-related death, with an estimated 604,100 new cases and 544,100 deaths annually [1, 2]. Despite advances in diagnostic and therapeutic strategies, the prognosis of patients with ESCA remains poor, with a 5-year survival rate of < 20% [1, 3, 4]. Current treatment modalities, including surgery, chemotherapy, and radiotherapy, are often limited by late-stage diagnosis, treatment resistance, and severe side effects [5–7]. Therefore, there is an urgent need to identify novel diagnostic biomarkers and therapeutic targets to improve patient outcomes.

In recent years, the role of molecular markers in cancer diagnosis and prognosis has garnered considerable attention. Unlike study markers, such as TP53 mutations, EGFR overexpression, or PD-L1, which are common in ESCA, minichromosome maintenance complex component 8 (MCM8) is involved in DNA replication and repair processes, introducing a unique perspective on tumor progression and treatment resistance. This new perspective addresses a major gap in ESCA research [8–10]. In the context of ESCA, the diagnostic and prognostic implications of *MCM8* expression remain largely unexplored. This study aims to fill this gap by investigating the expression patterns of *MCM8* in ESCA and evaluating its potential as a diagnostic and prognostic marker. We used bioinformatics tools to analyze gene expression data from The Cancer Genome Atlas (TCGA) and Gene Expression Omnibus (GEO) databases. Additionally, we explored the relationship between *MCM8* expression and overall survival (OS), disease-specific survival (DSS), and progression-free interval (PFI) in ESCA patients.

We examined the association between *MCM8* and N6-methyladenosine (m6a) methylation, a common RNA modification that has been implicated in cancer development and progression [11, 12]. We also analyzed the association of *MCM8* with genes related to angiogenesis, which plays an important role in the progression of esophageal cancer [13, 14]. Despite the known role of m6a methylation in cancer, there are few studies specifically linking this modification to ESCA and its interplay with angiogenesis. Finally, we constructed a competing endogenous RNA (ceRNA) network to elucidate the regulatory mechanisms underlying the role of *MCM8* in ESCA. We performed a comprehensive analysis of these processes, thereby providing a more holistic understanding of the molecular mechanisms associated with ESCA progression and a fresh approach to biomarker development.

The prognostic value of *MCM8* has been demonstrated in various cancers, including colorectal cancer and lung adenocarcinoma, in which high *MCM8* expression is associated with poor survival outcomes [15, 16]. In cancer cells, *MCM8* overexpression is associated with increased tumor aggressiveness and resistance to chemotherapeutic agents [17]. These findings suggest that *MCM8* plays a critical role in cancer progression and could serve as a valuable biomarker for predicting patient prognosis. Although the diagnostic and prognostic value of MCM8 has been demonstrated in multiple solid tumors, previous studies have not examined its regulatory mechanisms involving m6a modification or angiogenic pathways, particularly in the context of ESCA. This comparison highlights the contribution of our study to expanding the scope of MCM8 research and its potential therapeutic implications.

The present study provides valuable information on the diagnostic and prognostic value of *MCM8* in ESCA. We integrated gene expression analyses with survival data and explored the molecular mechanisms underlying the regulation of *MCM8* with the aim of contributing to the development of novel therapeutic strategies for ESCA. The research process is shown in Fig. 1.

Materials and methods

Public database

Clinical data and gene expression profiles were retrieved from The Cancer Genome Atlas (TCGA) database, which is accessible through the portal at http://portal.gdc.cancer.gov [18]. The dataset was expanded by collecting additional gene expression data from the Gene Expression Omnibus (GEO) database. Four distinct ESCA datasets were selected, namely GSE17351, GSE63941, GSE45168, and GSE45670, which are accessible via http://www.ncbi.nlm.nih.gov/geo [19]. These four GEO datasets contain human esophageal cancer samples and normal esophageal samples.

Gene expression analysis and survival outcome investigation in ESCA using bioinformatics tools

Differential gene expression analysis of TCGA ESCA dataset was performed using DESeq2 package within the R software environment [20], which identified genes with altered expression between normal and tumor groups. The thresholds for significance were set at a log-fold change (LogFC) > 1 and a p-value < 0.05. Differential gene expression analysis was performed on the four GEO datasets using the limma package [21], adhering to the same criteria for identifying differentially expressed genes (DEGs).

The prognostic significance of gene expression was examined using univariate Cox proportional hazards

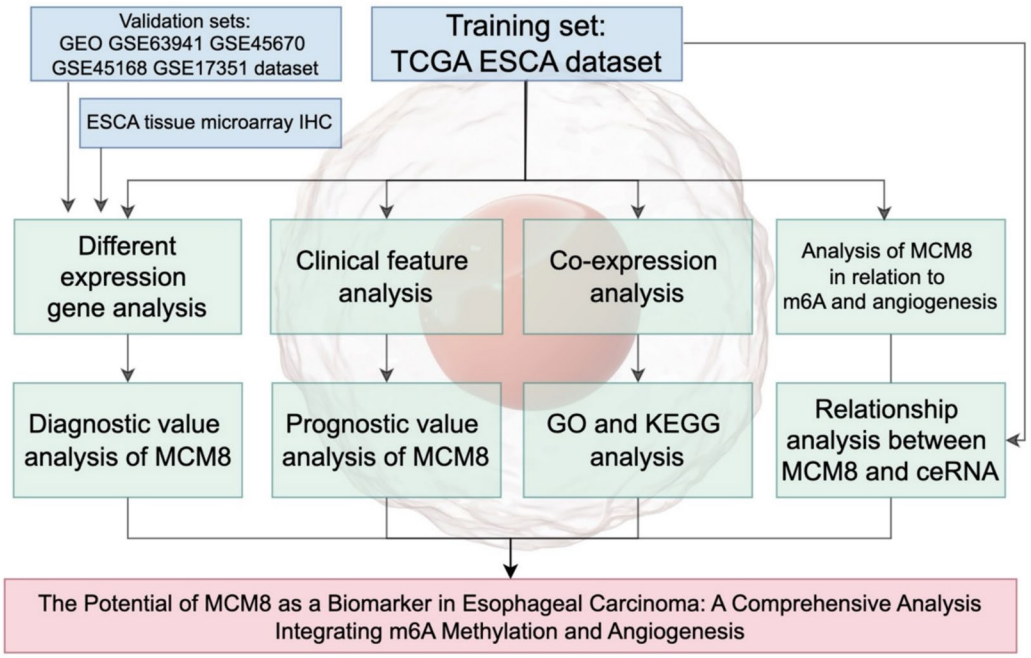

Fig. 1 Experimental design. The figure was created by Figdraw (www.figdraw.com)

regression analysis with the survival package in R, based on the expression levels of each gene in TCGA ESCA dataset. Prognostic relevance was assessed for OS, with hazard ratios (HR) > 1 and *p*-values < 0.05 indicating significance [22]. To visually represent the overlap of positively identified genes, we constructed an UpSet plot using the UpSetR package [23], which illustrates the intersection of DEGs across various datasets.

The ggplot2 package [24] was used to depict the expression differences of *MCM8* between normal and tumor groups in TCGA ESCA dataset, paired samples, and the four GEO datasets (GSE17351, GSE63941, GSE45168, and GSE45670), providing a comprehensive visual comparison of gene expression profiles.

Diagnostic and prognostic analysis of *MCM8* expression in ESCA

The diagnostic potential of *MCM8* expression in ESCA was examined by receiver operating characteristic (ROC) analysis using the pROC package in R. The sensitivity and specificity of *MCM8* as a diagnostic biomarker were determined, and the results were visualized using the ggplot2 package.

The prognostic significance of *MCM8* expression levels regarding different survival outcomes was assessed using the survival package. Proportional hazards assumption tests and fitted survival regression models were performed to explore the prognostic value of *MCM8* for DSS, OS, and progression-free interval (PFI). The outcomes were presented using a combination of the survminer and ggplot2 packages to provide a comprehensive visual representation of the survival data.

The correlation between *MCM8* expression levels and the clinical and pathological characteristics of ESCA patients was examined to assess the role of the gene in disease progression.

ESCA tissue microarray (TMA) and immunohistochemical staining

Human ESCA TMAs (48 tumor tissues, 48 paired paracancerous tissues) were purchased from Shanghai Zhuoli Biotechnology Co., Ltd. Immunohistochemical (IHC) staining was performed following an established protocol as previously described [25, 26]. Tissue samples were embedded in paraffin, sectioned, deparaffinized, and rehydrated, followed by IHC staining using rabbit anti-MCM8 polyclonal antibody. DAB was used for color development, followed by hematoxylin counterstaining. The stained sections were imaged under a light microscope to capture high-resolution images. Semi-quantitative analysis of the IHC staining images was performed using ImageJ software.

Correlation and functional enrichment analysis of *MCM8* co-expressed genes in ESCA

The co-expression network associated with *MCM8* in ESCA was examined using R software packages to analyze TCGA ESCA dataset. The correlation between *MCM8* and other genes was validated using the Pearson correlation coefficient, and associations were expressed by generating a volcano plot using the ggplot2 package. Heatmaps were constructed to display the top 20 genes positively and negatively correlated with *MCM8* [27]. Genes were selected for co-expression analysis based on a correlation threshold >0.5 and a p-value <0.05. Gene Ontology (GO) and Kyoto Encyclopedia of Genes and Genomes (KEGG) pathway analyses of the identified co-expressed genes was performed using the clusterProfiler package [28]. The results of these analyses were visualized using the ggplot2 package, providing a comprehensive overview of the biological processes and pathways associated with *MCM8*.

Analysis of *MCM8* in relation to m6a and angiogenesis

The correlation analysis module of the GEPIA online database (http://GEPIA.cancer-pku.cn/#correlation) [29] was used to explore the relationship between *MCM8* expression and key biological processes in ESCA, specifically focusing on m6a methylation and angiogenesis. The gene lists for m6a and angiogenesis were curated based on previous studies [30, 31]. The correlation between *MCM8* expression levels and genes related to ESCA m6a and angiogenesis from TCGA ESCA and GSE45670 datasets was analyzed using Pearson's correlation. Potential associations between *MCM8* expression and the indicated biological processes were visualized by constructing co-expression heatmaps using the ggplot2 package. Genes showing consistent correlations in both datasets were identified and their co-expression patterns were visualized using ggplot2. Samples were stratified according to the median expression level of *MCM8* to investigate the differential expression of m6a and angiogenesis-related genes between high and low expression groups.

Predictive analysis and ceRNA network construction for *MCM8* in ESCA

MicroRNAs (miRNAs) targeting *MCM8* were identified using miRWalk (http://mirwalk.umm.uni-heidelberg.de/) and MicroT-CDS (https://dianalab.e-ce.uth.gr/html/dianauniverse/index.php?r=microT_CDS) [32]. We performed a systematic prediction followed by a differential expression analysis to confirm and refine the list of candidate miRNAs.

Long non-coding RNAs (lncRNAs) that may serve as targets for the identified miRNAs were predicted using ENCORI (https://rnasysu.com/encori/index.php) [33] and miRNet (https://www.mirnet.ca/miRNet/home.xhtml) [34]. Differential expression analysis was performed to confirm the final set of lncRNAs with significant regulatory potential.

Building upon the ceRNA hypothesis, which posits that mRNAs, miRNAs, and lncRNAs can interact through shared miRNA response elements, we constructed a comprehensive ceRNA network. The interactions within this network were verified using RNAhybrid online tool (https://bibiserv.cebitec.uni-bielefeld.de/rnahybrid?id=rnahybrid_view_submission) [35] to predict potential binding sites between mRNAs and miRNAs, as well as between lncRNAs and miRNAs, thereby providing a molecular basis for the observed ceRNA relationships.

Statistical analysis

Statistical analyses were performed using R software. All computations were performed with strict adherence to established statistical methods, thereby ensuring the reliability and validity of the results. The Xiantao online tool (https://www.xiantaozi.com/) was used for data visualization, which facilitated the generation of graphical representations of the statistical outcomes. Statistical significance was determined using a threshold of $p < 0.05$.

Results

Identification and analysis of differentially expressed genes in ESCA with a focus on *MCM8*

To identify deregulated genes in ESCA, we performed a comprehensive analysis of TCGA ESCA dataset and four datasets from GEO using stringent filtering criteria as previously described. The differential gene expression analysis identified 4912 dysregulated genes in the TCGA ESCA dataset, 1081 in GSE17351, 2875 in GSE63941, 1436 in GSE45168, and 1537 in GSE45670. These findings were refined by prognostic selection analysis, which identified 517 genes in the TCGA ESCA dataset that met the established criteria. An UpSet plot indicated that the *MCM8* and *E2 F7* genes consistently met the screening criteria across the six datasets (Fig. 2a). *E2 F7* has been reported previously in the context of ESCA, whereas the involvement of *MCM8* has not been reported extensively, leading us to focus on *MCM8* for further investigation.

Figure 2b–g shows the differential expression of *MCM8*, indicating that the expression of the gene was consistently higher in tumor groups than in normal groups in TCGA ESCA dataset, paired samples, and the four GEO datasets (GSE17351, GSE63941, GSE45168, and GSE45670). This supports the potential of *MCM8* as a biomarker in ESCA ($p < 0.05$).

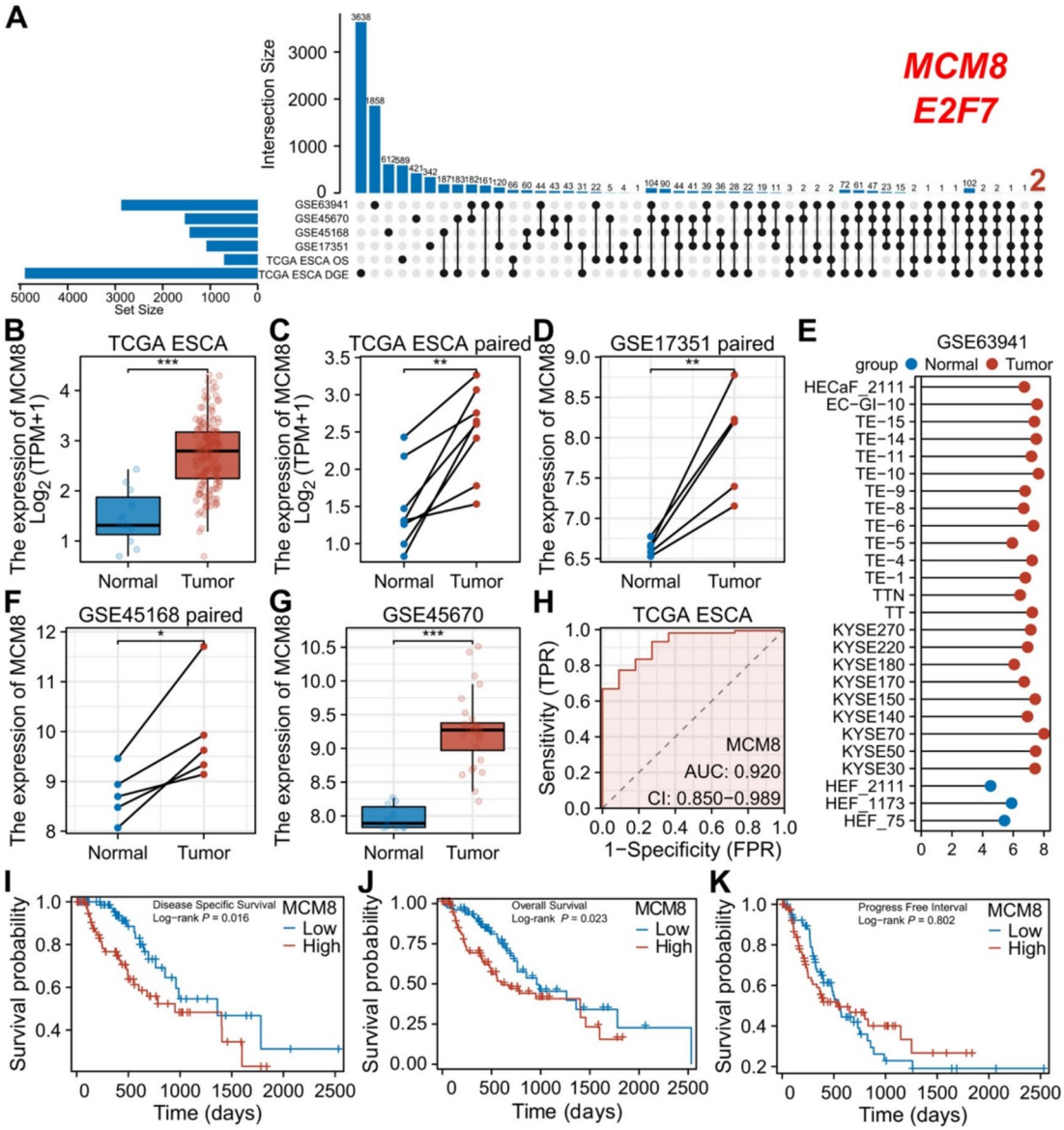

Fig. 2 Identification and analysis of differentially expressed genes in ESCA with focus on *MCM8*. **a** UpSet Plot illustrating the overlap of genes meeting the screening criteria for differential expression and prognostic value across six datasets, including TCGA ESCA dataset and GEO datasets GSE17351, GSE63941, GSE45168, and GSE45670. **b–g** Plots illustrating the differential expression of *MCM8* in tumor groups relative to normal groups in various datasets. **h** Receiver Operating Characteristic (ROC) curve for *MCM8*, highlighting its significant diagnostic value in ESCA with an AUC of 0.920 [95% confidence interval (CI), 0.850–0.989; $p < 0.05$]. **i, j** Kaplan–Meier survival curves demonstrating the association between elevated *MCM8* expression and poorer overall survival (OS) and disease-specific survival (DSS) ($p < 0.05$). **k** Kaplan–Meier survival curve for the progression-free interval (PFI) ($p > 0.05$)

Diagnostic and prognostic value of *MCM8* expression in ESCA

To further examine the diagnostic efficacy of *MCM8* in ESCA, we constructed ROC curves and calculated the area under the curve (AUC). ROC analysis supported the diagnostic value of *MCM8* in ESCA, with an AUC of 0.920 (confidence interval, 0.850–0.989; $p < 0.05$) (Fig. 2h).

A previous univariate Cox analysis indicated that *MCM8* (HR = 1.77, $p < 0.05$) was statistically significant. The prognostic significance of *MCM8* expression for different survival metrics was assessed using the Kaplan–Meier plotter. The findings indicated that elevated *MCM8* expression was correlated with poorer OS and DSS (Fig. 2i, j, $p < 0.05$). However, no statistically

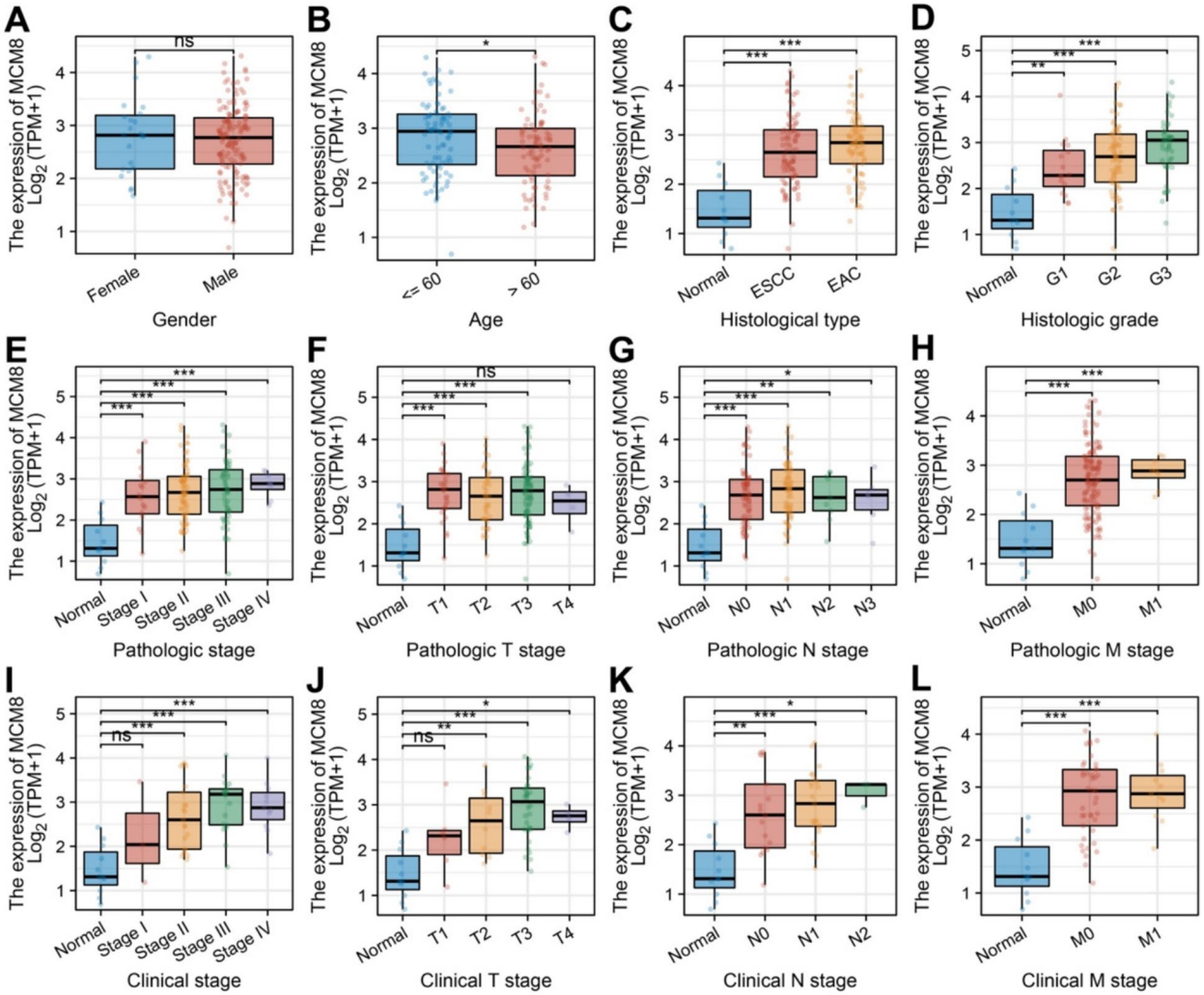

Fig. 3 Correlation of *MCM8* expression with clinical characteristics in ESCA. **a** There was no significant association between *MCM8* expression and gender ($p > 0.05$). **b**–**l** Plots illustrating the significant correlation of *MCM8* expression with age, histological subtype, histological grade, and staging systems for both pathology and clinical presentation, covering T, N, and M categories ($p < 0.05$)

significant association was observed between *MCM8* expression and PFI (Fig. 2k, $p > 0.05$).

Analysis of the correlation between *MCM8* expression and various clinical characteristics showed that *MCM8* expression was not associated with gender (Fig. 3a, $p > 0.05$), whereas it was significantly linked to age, histological subtype, histological grade, and the staging systems for both pathology and clinical presentation, encompassing T, N, and M categories (Fig. 3b–l, $p < 0.05$).

MCM8 is overexpressed in ESCA tissues

The expression of *MCM8* in ESCA was further examined using a TMA and IHC staining (Fig. 4a). The results showed that the *MCM8* protein is predominantly expressed in the cytoplasm. Statistical analysis demonstrated that MCM8 was significantly overexpressed in ESCA tissue samples compared with adjacent non-cancerous tissues (Fig. 4b, $p < 0.05$). However, *MCM8* expression was not associated with age or gender (Fig. 4c, d, $p > 0.05$).

Correlation and functional enrichment analysis of *MCM8* in ESCA reveals potential biological roles

To gain insight into the biological roles of *MCM8* in ESCA, we examined the relationship between *MCM8* and all genes in TCGA ESCA dataset using Pearson's correlation. Protein-coding genes were analyzed using a correlation threshold $|cor| > 0.3$ and a p-value < 0.05, which

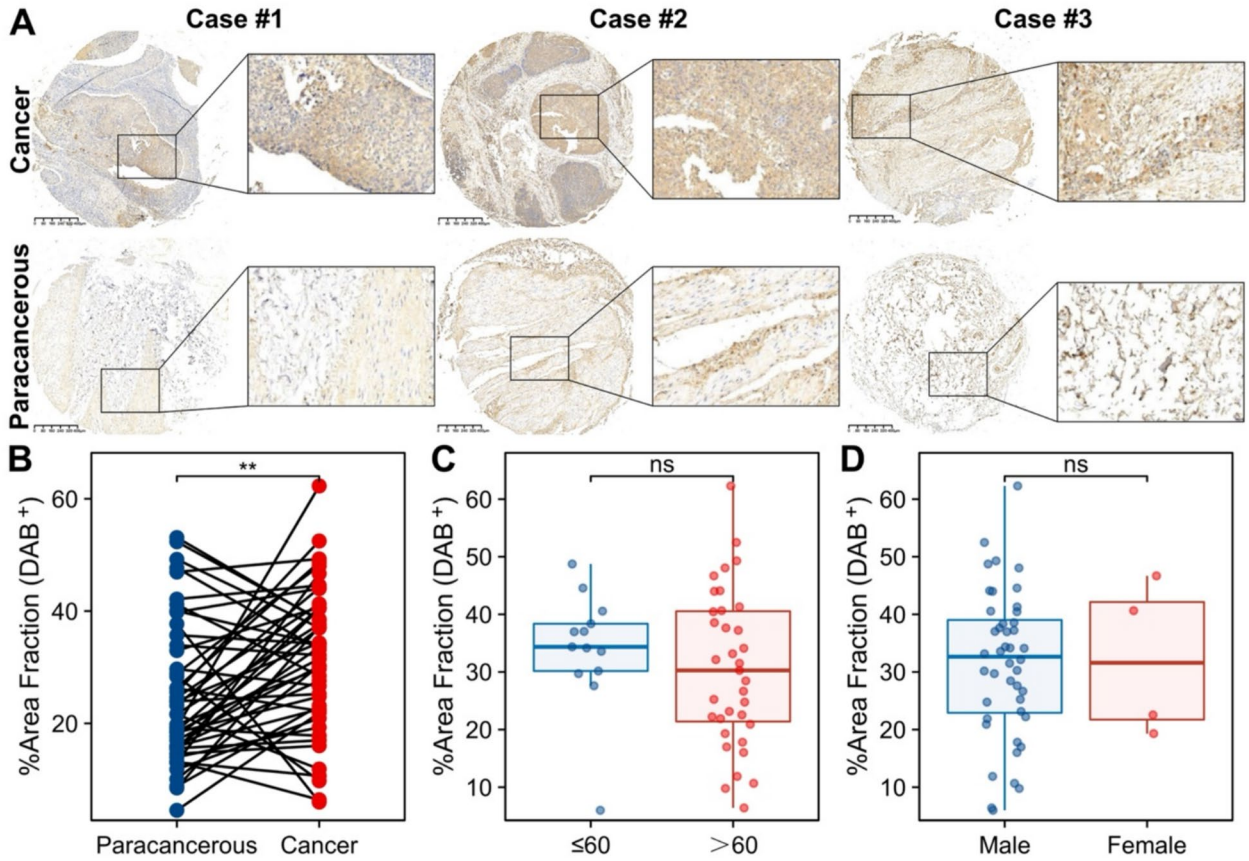

Fig. 4 Immunohistochemical analysis of *MCM8* expression in ESCA. **a** Representative images of tissue microarray (TMA) sections showing *MCM8* protein expression, which was predominantly localized to the cytoplasm. **b** *MCM8* was significantly overexpressed in ESCA tissues compared with adjacent normal tissues ($p < 0.05$). **c, d** No significant association was observed between *MCM8* expression and patient age or gender ($p > 0.05$)

led to the identification of 4341 genes that were positively correlated with *MCM8* and 30 genes that were negatively correlated. Among these, POLR3 F showed the strongest positive correlation with *MCM8*, whereas PLEKHN1 had the most significant negative correlation (Fig. 5a).

A visual synopsis of these correlations was achieved by generating heatmaps to display the top 20 genes with the highest positive (Fig. 5b) and negative (Fig. 5c) correlations with *MCM8*. A higher correlation threshold of cor > 0.5 and $p < 0.05$ narrowed down the selection to 621 co-expressed genes. These genes, along with *MCM8*, underwent further functional enrichment analysis using the GO and KEGG databases. We used an adjusted *p*-value cutoff of p.adj < 0.05 and identified 649 pathways, including 453 biological processes, 107 cellular components, 75 molecular functions, and 14 KEGG pathways. The findings indicate that *MCM8* and its co-expressed genes may participate in crucial biological processes such as DNA replication, kinetochore, ATP-dependent activity, acting on DNA, and the Fanconi anemia pathway (Fig. 5d).

Correlation between *MCM8* expression and m6a methylation in ESCA

The potential association between *MCM8* expression and the m6a methylation machinery in ESCA was examined by correlation analysis using the GEPIA online tool. The results showed a significant positive correlation between *MCM8* expression and a panel of 20 m6a-associated genes (Fig. 6a, $p < 0.05$). Analysis of TCGA ESCA dataset confirmed this association, showing a positive correlation between *MCM8* and the expression of these 20 m6a genes (Fig. 6b, $p < 0.05$). In the GSE45670 dataset, *MCM8* was significantly positively correlated with the expression of *HNRNPA2B1*, *RBMX*, and *YTHDF1* (Fig. 6c, $p < 0.05$). The significant positive correlation between *MCM8* and the m6a genes *HNRNPA2B1*, *RBMX*, and *YTHDF1* in the two datasets was visualized using scatter plots (Fig. 6d).

Further exploration of TCGA ESCA dataset identified 18 m6a genes with significantly different expression between high and low *MCM8* expression groups, including *ALKBH5*, *FTO*, *HNRNPA2B1*, *HNRNPC*, *IGF2BP1*,

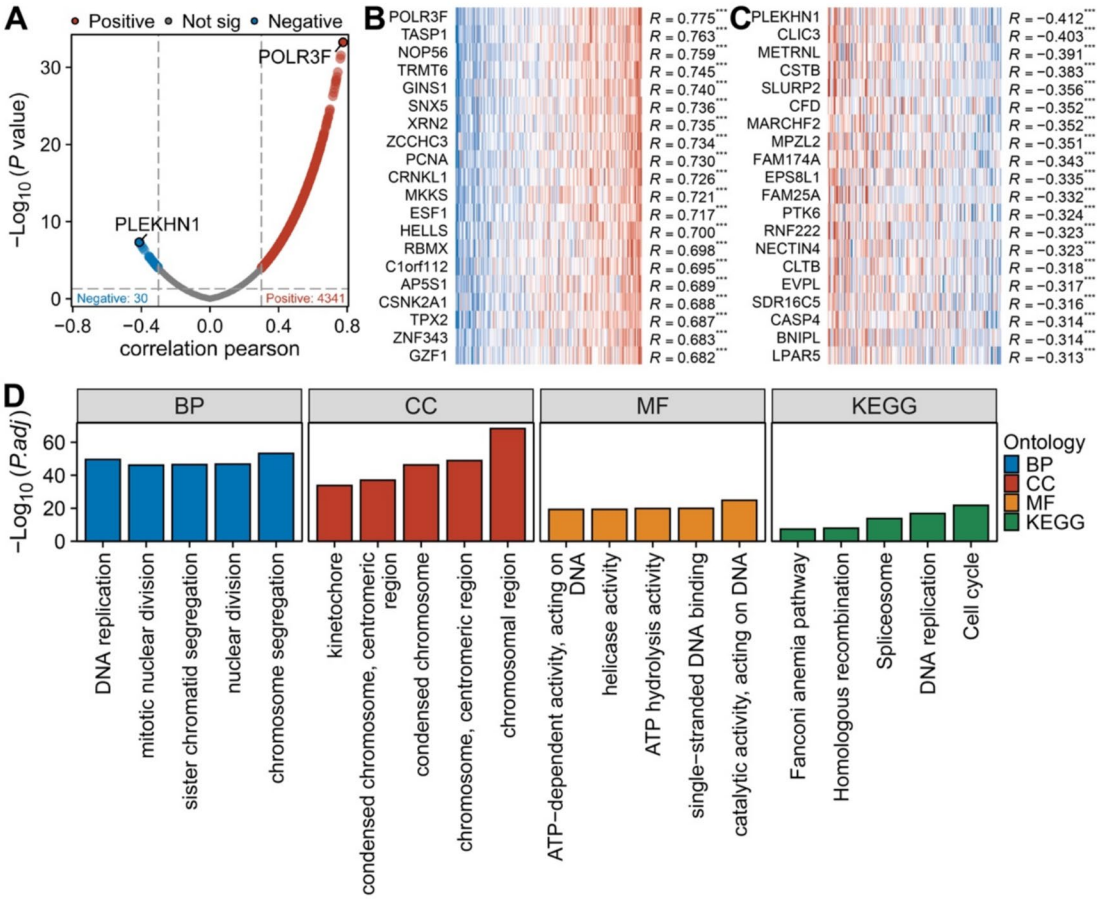

Fig. 5 Correlation and Functional Enrichment Analysis of *MCM8* in ESCA. **a** Volcano plots with a Pearson correlation coefficient indicating the strength and significance of the relationship between *MCM8* and other protein-coding genes within TCGA ESCA dataset. Highlighted are POLR3 F with the highest positive correlation and PLEKHN1 with the most significant negative correlation with *MCM8*. **b, c** Heatmaps depicting the top 20 genes with the highest positive and negative correlations with *MCM8*, respectively. These visualizations provide an overview of the gene expression patterns closely associated with *MCM8* levels. **d** Enrichment analysis of *MCM8* co-expressed genes was performed using Gene Ontology (GO) terms and the Kyoto Encyclopedia of Genes and Genomes (KEGG)

IGF2BP2, *IGF2BP3*, *METTL14*, *METTL3*, *RBM15*, *RBM15B*, *RBMX*, *VIRMA*, *WTAP*, *YTHDC1*, *YTHDF1*, *YTHDF3*, and *ZC3H13* (Fig. 6e). However, the GSE45670 dataset showed significant expression differences between the high and low *MCM8* expression groups for only two m6a genes, *HNRNPA2B1* and *YTHDF1* (Fig. 6f). A Venn diagram was drawn to illustrate the positive association of *HNRNPA2B1* and *YTHDF1* with *MCM8* expression (Fig. 6g).

Association between *MCM8* expression and angiogenesis in ESCA

The association between *MCM8* expression and angiogenesis in ESCA was examined by correlation analysis using the GEPIA online tool. This analysis was designed to encompass a broad spectrum of genes known to participate in angiogenesis, a critical hallmark of cancer progression. The results showed a significant positive correlation between *MCM8* and the expression patterns of 36 angiogenesis-related genes, suggesting a potential regulatory role of *MCM8* in this process (Fig. 7a, $p < 0.05$). We expanded the analysis to TCGA ESCA dataset and observed a consistent positive correlation between *MCM8* and the expression of 15 angiogenesis-related genes, including *APOH*, *APP*, *CXCL6*, *FGFR1*, *FSTL1*, *ITGAV*, *LRPAP1*, *PDGFA*, *PGLYRP1*, *PRG2*, *PTK2*, *SERPINA5*, *VAV2*, *VCAN*, and *VTN* (Fig. 7b, $p < 0.05$). The correlation was more pronounced in TCGA dataset, supporting the involvement of *MCM8* in angiogenesis in ESCA. By contrast, the GSE45670 dataset revealed a significant positive correlation predominantly between *MCM8* and PTK2 (Fig. 7b, $p < 0.05$). Scatter plots were utilized to visually represent the significant positive correlation between *MCM8* and PTK2 in both datasets

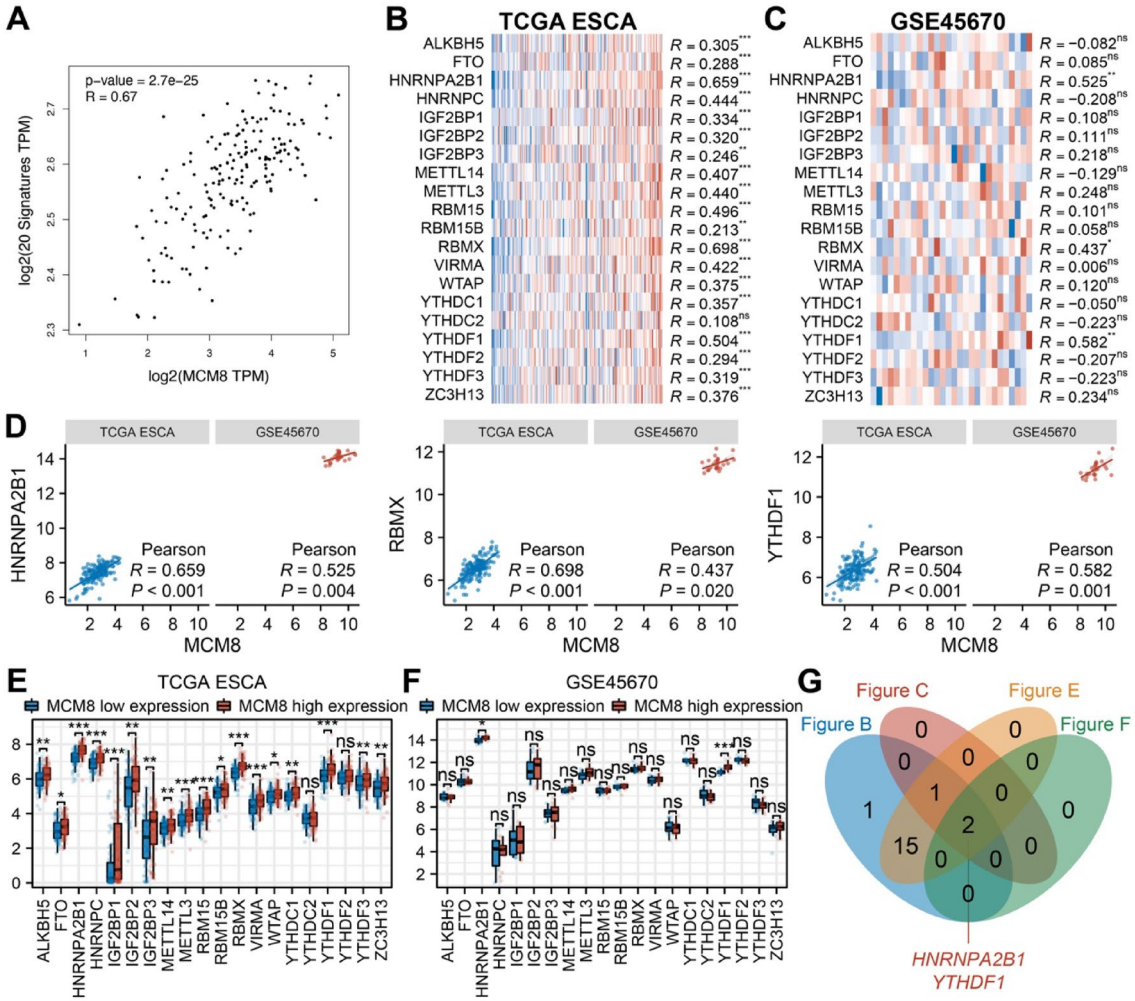

Fig. 6 Correlation analysis of *MCM8* expression with m6a methylation genes in ESCA. **a** Correlation plot from the GEPIA online tool demonstrating a significant positive correlation between *MCM8* expression and a panel of 20 m6a-associated genes in ESCA ($p < 0.05$). **b** Heat map illustrating the consistent positive correlation between *MCM8* and the 20 m6a genes in TCGA ESCA dataset ($p < 0.05$). **c** Heat plot highlighting the significant positive correlation of *MCM8* expression with *HNRNPA2B1*, *RBMX*, and *YTHDF1* in the GSE45670 dataset ($p < 0.05$). **d** Scatter plots displaying the significant positive correlation between *MCM8* and the m6a genes *HNRNPA2B1*, *RBMX*, and *YTHDF1* in TCGA and GSE45670 datasets. **e** Bar chart showing the significant differential expression of 18 m6a genes in TCGA ESCA dataset between high and low *MCM8* expression groups. **f** Bar chart indicating significant expression differences for two m6a genes, *HNRNPA2B1* and *YTHDF1*, between high and low *MCM8* expression groups in the GSE45670 dataset. **g** Venn diagram illustrating the positive association of *HNRNPA2B1* and *YTHDF1* with *MCM8* expression levels in the analyzed datasets

and to confirm the differential expression of these genes between high and low *MCM8* expression groups (Fig. 7c, d).

MCM8-miRNA regulatory axis in ESCA

Evidence suggests that the aberrant regulation of ceRNA networks contributes to tumorigenesis and cancer progression. In this study, we aimed to predict and construct an *MCM8*-centered ceRNA network in ESCA. Analysis of the miRWalk and MicroT-CDS databases identified 2179 and 60 miRNAs, respectively, predicted to interact with *MCM8*, and a Venn diagram identified a subset of 37 miRNAs present in both databases that could be involved in the regulation of *MCM8* (Fig. 8a). Expression analysis of these miRNAs in TCGA ESCA dataset showed that seven miRNAs were upregulated and two were downregulated in tumor samples compared with normal controls (Fig. 8b). The upregulated miRNAs included hsa-miR-105 -5p (LogFC = 6.87, p = 6.134e− 14), hsa-miR- 335 -3p (LogFC = 1.73, p = 1.196e− 07), hsa-miR- 940 (LogFC = 1.63, p = 3.577e− 05), hsa-miR- 942 -3p (LogFC = 1.48, p = 0.003), hsa-miR- 135b- 5p (LogFC = 2.13,

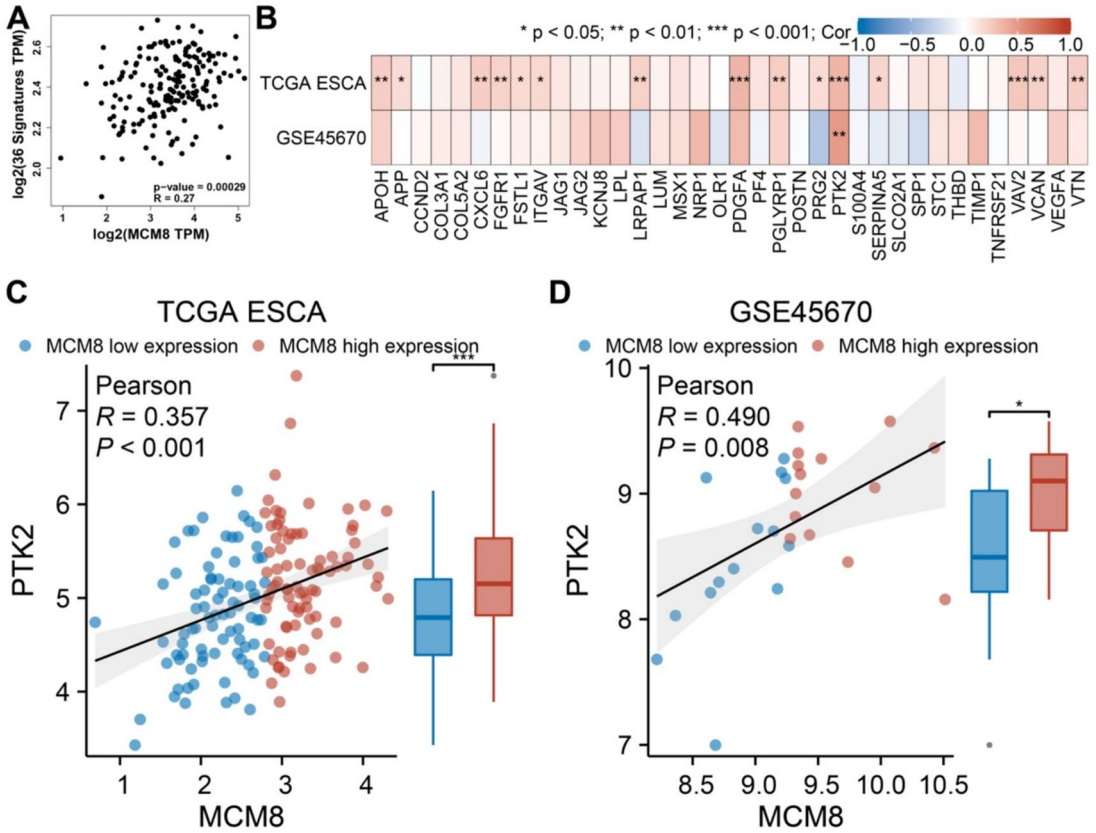

Fig. 7 Analysis of the correlation between *MCM8* expression and angiogenesis-related genes in ESCA. **a** Correlation plot illustrating the significant positive association between *MCM8* expression and a panel of 36 angiogenesis-related genes in ESCA samples, as determined by the GEPIA online tool ($p < 0.05$). **b** Heat map and associated statistical analysis from TCGA ESCA dataset showing a consistent positive correlation between *MCM8* and the expression of 15 angiogenesis-related genes ($p < 0.05$). Heat plot highlighting the predominant significant positive correlation between *MCM8* and PTK2 expression in the GSE45670 dataset ($p < 0.05$). **c, d** Scatter plots show angiogenesis-related genes (PTK2) significantly positively correlated with *MCM8* expression levels in TCGA and GSE45670 datasets and confirm that the expression of PTK2 is also significantly different between the high and low *MCM8* expression groups

$p = 1.360e-07$), hsa-miR- 1304 -3p (LogFC = 3.58, $p = 4.606e-05$), and hsa-miR- 6783 -3p (LogFC = 1.27, $p = 0.048$), whereas hsa-miR- 135a- 5p (LogFC = − 3.13, $p = 6.317e-07$) and hsa-miR- 202 -5p (LogFC = − 2.92, $p = 2.539e-05$) were downregulated, suggesting a potential reciprocal relationship with the overexpression of *MCM8* mRNA in tumor tissues. Guided by the ceRNA hypothesis, which posits that mRNAs overexpressed in tumors correspond to the downregulation of targeting miRNAs, we selected hsa-miR- 135a- 5p and hsa-miR- 202 -5p as candidate miRNAs for targeting *MCM8*. Their reduced expression in tumor samples was further confirmed (Fig. 8c, e). Bioinformatics analysis using RNAhybrid identified potential binding sites between *MCM8* and the two miRNAs, providing molecular evidence for their interaction (Fig. 8d, f).

LncRNA-miRNA interactions in the *MCM8* ceRNA network

To further examine the network of ceRNAs associated with *MCM8* in ESCA, we analyzed lncRNAs that may interact with hsa-miR- 135a- 5p. A search of the ENCORI and miRNet databases identified 27 and 37 lncRNAs, respectively, predicted to interact with hsa-miR- 135a- 5p. Eight lncRNAs (GAS5, DANCR, PURPL, RPARP-AS1, NEAT1, MALAT1, OIP5-AS1, and XIST) were common to the two databases (Fig. 9a). Differential expression analysis in TCGA ESCA dataset showed that PURPL (log2 FC = 1.61, $p = 0.041$) was the only lncRNA showing a significant difference in expression (Fig. 9b), and its upregulation in tumor samples compared with normal samples was confirmed (Fig. 9c). Bioinformatics analysis using RNAhybrid identified potential binding sites between PURPL and hsa-miR- 135a- 5p, suggesting a direct molecular interaction (Fig. 9d).

Parallel analysis of lncRNAs targeting hsa-miR- 202 -5p yielded 14 and 13 lncRNAs from the ENCORI

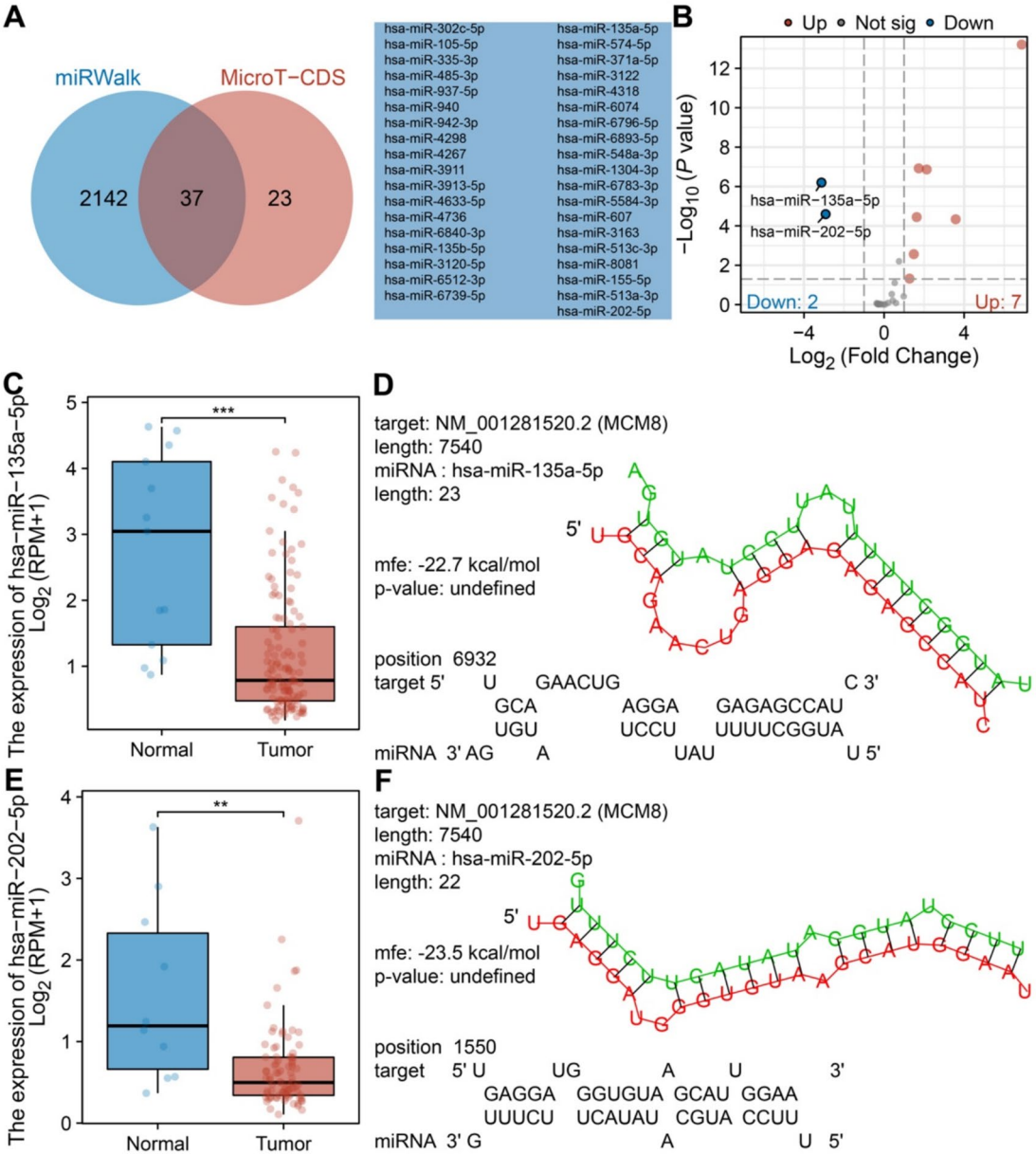

Fig. 8 *MCM8*-miRNA regulatory axis in ESCA. **a** Venn diagram displaying the intersection of 37 miRNAs predicted to interact with *MCM8*, as identified by the miRWalk and MicroT-CDS databases. **b** Volcano chart of the differential expression of the 37 intersecting miRNAs in TCGA ESCA dataset showing the seven upregulated (hsa-miR- 105 - 5p, hsa-miR- 335 - 3p, hsa-miR- 940, hsa-miR- 942 - 3p, hsa-miR- 135b- 5p, hsa-miR- 1304 - 3p, hsa-miR- 6783 - 3p) and two downregulated (hsa-miR- 135a- 5p, hsa-miR- 202 - 5p) miRNAs in tumor samples compared with normal controls. **c** Expression of hsa-miR- 135a- 5p in tumor versus normal samples from TCGA ESCA dataset confirming its downregulation in tumor tissues. **d** Bioinformatics analysis using RNAhybrid depicting the potential binding site between *MCM8* and the downregulated miRNA hsa-miR- 135a- 5p. **e** Expression of hsa-miR- 202 - 5p corresponding to the downregulation of hsa-miR- 135a- 5p in tumor samples. **f** RNAhybrid analysis identified the potential binding site between *MCM8* and the downregulated miRNA hsa-miR- 202 - 5p

and miRNet databases, respectively, with 3 lncRNAs (HCG11, EBLN3P, and NORAD) common to both databases (Fig. 9e). However, the expression of these lncRNAs did not differ significantly between tumor and normal samples, leading to their exclusion from further analysis (Fig. 9f).

Taken together, the findings indicate that PURPL may act as a competitive ceRNA for hsa-miR- 135a- 5p, potentially promoting the expression of *MCM8*. These

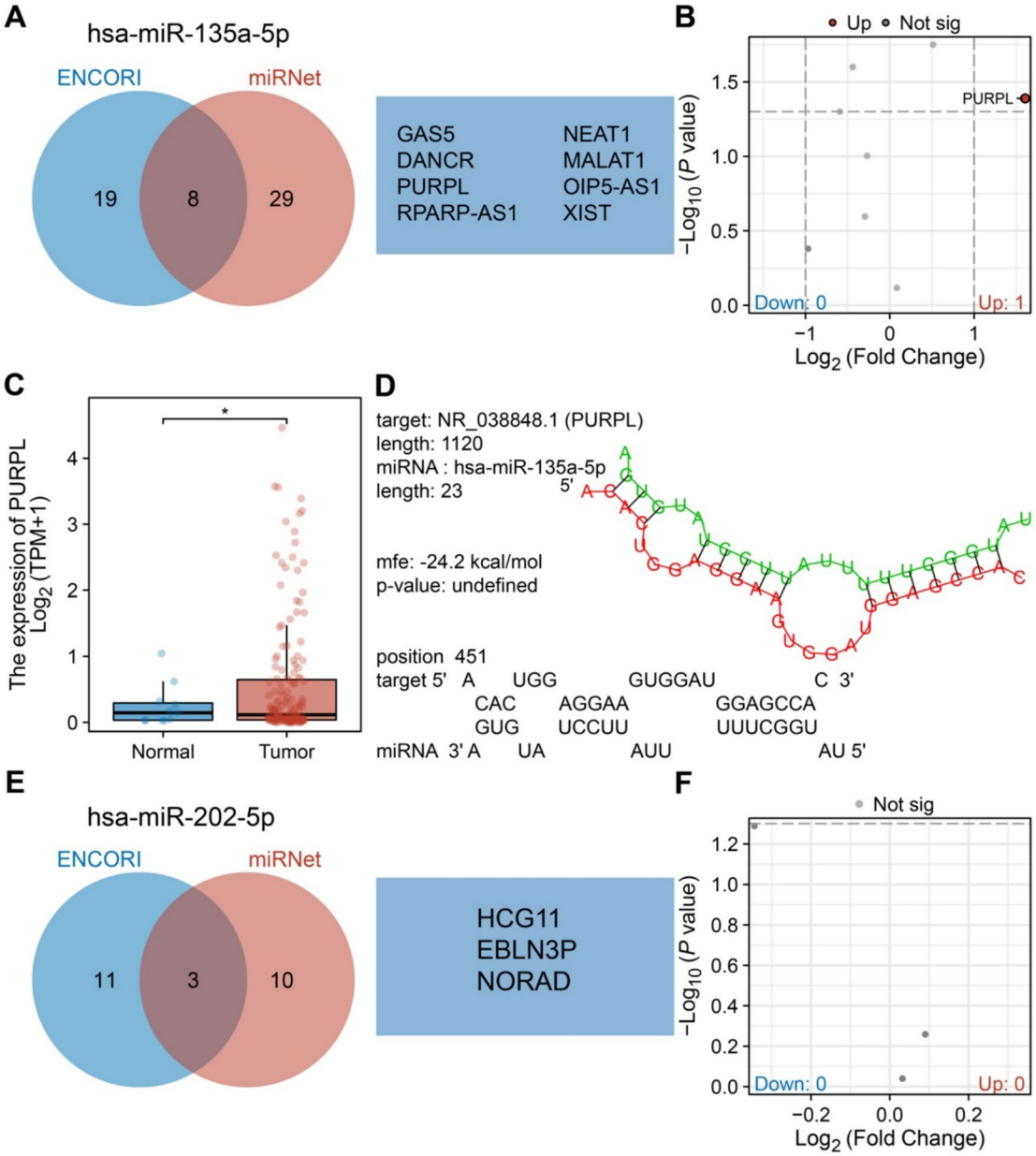

Fig. 9 Comprehensive analysis of lncRNAs in the *MCM8* ceRNA network in ESCA. **a** Venn diagram showing the intersection of lncRNAs predicted to interact with hsa-miR- 135a- 5p, as identified by the ENCORI and miRNet databases. **b** Volcano chart from TCGA ESCA dataset showing the differential expression of the intersecting lncRNAs; PURPL was identified as the only lncRNA significantly upregulated in tumor samples. **c** Validation plot confirming the specific upregulation of PURPL in tumor versus normal samples in TCGA ESCA dataset. **d** Bioinformatics analysis using RNAhybrid shows the potential binding sites between PURPL and hsa-miR- 135a- 5p, suggesting direct molecular interaction. **e** Venn diagram representing the overlap of lncRNAs predicted to interact with hsa-miR- 202 - 5p, as identified by the ENCORI and miRNet databases. **f** Expression analysis of the lncRNAs targeting hsa-miR- 202 - 5p shows no significant differences in expression between tumor and normal samples, resulting in their exclusion from further analysis

data may contribute to our understanding of the role of *MCM8* and its ceRNA network in the pathogenesis of ESCA.

Discussion

ESCA is a highly aggressive malignancy characterized by high morbidity and mortality rates, which poses a substantial threat to global health. It is the sixth leading cause of cancer-related death worldwide, and its incidence is

particularly high in certain regions such as East Asia [1, 2]. The prognosis of patients with ESCA remains poor, which is primarily due to late-stage diagnosis and limited effective treatment options. The aggressive nature of this cancer and its tendency towards early metastasis further complicate treatment efforts, underscoring the need to identify effective diagnostic and prognostic biomarkers to improve early detection and treatment efficacy [36–40].

ESCA is characterized by rapid progression and a high rate of recurrence, which contribute to its poor survival rates [2, 41]. Advances in molecular biology and bioinformatics techniques have opened new avenues for understanding the complex genetic and epigenetic landscape of ESCA. For instance, studies show that the expression of specific genes and non-coding RNAs can significantly impact the progression of ESCA [42, 43]. The integration of bioinformatics tools for analyzing gene expression and the identification of key regulatory networks can uncover novel therapeutic targets. This research direction is promising for developing personalized treatment strategies and improving patient outcomes [26, 44]. Comprehensive analysis of the molecular mechanisms underlying ESCA, such as the role of *MCM8* and its interaction with m6a methylation and angiogenesis, may provide insight into the pathogenesis of the disease and suggest potential interventions.

The *MCM8* gene encodes a member of the mini-chromosome maintenance (MCM) protein family, which plays a crucial role in the initiation of DNA replication. Although significant progress has been made in identifying molecular markers such as TP53 mutations, EGFR overexpression, and PD-L1 expression, these markers often lack specificity or are not entirely applicable to clinical practice for early diagnosis or the design of personalized treatments. The involvement of MCM8 in DNA replication and repair provides a new perspective, particularly because of its association with epigenetic mechanisms such as m6a methylation and angiogenic pathways, which have not been analyzed in detail in ESCA. In this study, we showed that *MCM8* was significantly overexpressed in ESCA tissues compared with normal tissues, and this overexpression was associated with poorer OS and DSS. The high diagnostic potential of *MCM8*, as evidenced by an AUC of 0.920, underscores its value as a biomarker for ESCA. Pearson correlation analysis revealed that *MCM8* is co-expressed with multiple genes involved in critical biological processes such as DNA replication and cell cycle regulation. The significant positive correlation between *MCM8* and m6a methylation-related genes suggests that *MCM8* may influence ESCA progression through epigenetic modifications. Additionally, ceRNA network analysis indicated that miRNAs such as hsa-miR- 135a- 5p and hsa-miR- 202 -5p, which target *MCM8*, are downregulated in tumor samples, potentially leading to *MCM8* overexpression. The overexpression of *MCM8* and its prognostic value have been demonstrated in several malignancies such as bladder, cervical, colorectal, hepatocellular, gastric, and pancreatic cancers [15, 45–49]. The consistency of these findings across various cancer types supports the involvement of *MCM8* in cancer progression and its potential as a target for therapeutic intervention.

In this study, we identified several DEGs in ESCA in multiple datasets, and *MCM8* was identified as a key gene of interest due to its elevated expression in tumor tissues compared with normal tissues. Enrichment analysis indicated that *MCM8* is involved in several crucial biological processes and pathways such as DNA replication, kinetochore, ATP-dependent activity, acting on DNA, and the Fanconi anemia pathway. These processes are essential for maintaining genomic stability and proper cell division, and they play an important role in the etiology and progression of oncogenic processes [50–52]. The interaction between *MCM8* and the cellular machinery that regulates genomic stability and cell division suggests a complex regulatory network in which *MCM8* dysregulation could have a significant impact on cancer cell behavior.

We found a positive correlation between *MCM8* and genes related to the m6a methylation machinery, including *HNRNPA2B1* and *YTHDF1*. m6a methylation is an important post-transcriptional modification involved in the regulation of mRNA stability, alternative splicing, and translational efficiency, thereby influencing a multitude of cellular functions. In the context of ESCA, Guo et al. described the role of *HNRNPA2B1* as an oncogenic driver in ESCA, promoting tumor progression by upregulating the lipogenic enzymes *ACLY* and *ACC1* [53]. In previous work, we identified *YTHDF1* as a prognostic biomarker in ESCA and demonstrated its involvement in immune cell infiltration, glycolytic regulation, ferroptosis, and the ceRNA network [54]. The observed association of *MCM8* with these m6a-related genes suggests that its role in ESCA involves the modulation of m6a methylation, thereby impacting gene expression patterns and contributing to the interplay of molecular mechanisms underlying ESCA pathogenesis. This interconnection underscores the intricate regulatory networks within the cancer cell and the potential for *MCM8* as a node in these pathways, influencing both the epigenetic and transcriptional profiles in the disease context.

Angiogenesis, the process of new blood vessel formation, is a cardinal mechanism involved in tumor growth and metastasis, as it provides cancer cells with the blood supply essential for growth and dissemination [13, 14]. We found a significant positive correlation between

MCM8 and the angiogenesis-associated gene *PTK2*. Feng et al. showed that HMGB1-induced overexpression of *KLF7* promotes liver cancer progression and metastasis through the upregulation of *TLR4* and *PTK2*. This observation together with the present findings suggests a mechanistic convergence in which *MCM8* may be implicated in angiogenesis-related pathways. *MCM8* could contribute to tumor progression by fostering the development of new vasculature, thereby providing a conducive environment for the nourishment and spread of neoplastic cells.

ceRNA networks play an important role in the development of ESCA [55–57]. We identified several miRNAs, such as hsa-miR- 135a- 5p and hsa-miR- 202 - 5p, that were downregulated in tumor samples and negatively correlated with *MCM8* expression. This finding aligns with the ceRNA hypothesis by which downregulation of these miRNAs leads to the upregulation of their target gene, *MCM8*. We also showed that the lncRNA PURPL increases *MCM8* expression by sequestering hsa-miR- 135a- 5p, thereby reducing its inhibitory effect on *MCM8*. Wang et al. found that the lncRNA RP11 - 197 K6.1 is significantly upregulated in colorectal cancer tissues and cell lines and promotes cancer cell migration and metastasis by interacting with miR- 135a- 5p, thereby promoting tumor growth by suppressing the inhibition of DLX5 expression [58]. Berhane et al. found that knockout of PURPL inhibits the proliferation of liver cancer cells, induces apoptosis, and sensitizes tumor cells to treatment with the chemotherapy agent doxorubicin [59]. This study supports that ceRNA networks involving *MCM8* may play an important role in the progression of ESCA.

In summary, this study highlights the multifaceted role of *MCM8* in ESCA including its involvement in m6a methylation and angiogenesis. The construction of the ceRNA network provides further insight into the regulatory mechanisms underlying *MCM8* expression. These findings underscore the potential of *MCM8* as a diagnostic and prognostic biomarker and as a therapeutic target in ESCA.

Conclusion

In this study, we performed comprehensive bioinformatics analyses and elucidated the role of *MCM8* in ESCA. We showed that *MCM8* is expressed at high levels in ESCA and its overexpression is associated with poor OS. ROC analysis supported the potential of *MCM8* as a diagnostic biomarker. We found that *MCM8* is correlated with genes related to m6a methylation and angiogenesis, providing insight into its possible regulatory mechanisms. The construction of a ceRNA network involving *MCM8* offers a new perspective on its role in ESCA. Future studies should focus on validating these findings through experimental studies and clinical trials to fully elucidate the diagnostic and prognostic potential of *MCM8* in ESCA.

Acknowledgements
Not applicable.

Author contributions
X.-S.L.: Conceptualization, Methodology, Writing—Original Draft. Y.X.: Software, Validation. L.-S.D.: Software, Validation. A.L.: Validation. J.L.: Validation. Y.Z.: Validation. J.X.: Supervision. Z.-J.P.: Supervision, Writing—Review & Editing.

Funding
This work was supported by the Hubei Provincial Natural Science Foundation of China (2024AFD284), Hubei Provincial Clinical Research Center for precision Diagnosis and Treatment of Liver Cancer Open Fund (2024LCOF08), Innovative Research Program for Graduates of Hubei University of Medicine (grant no. YC2024042), the Shiyan Taihe Hospital hospital-level project (2024JJXM087), and the Key Discipline Project of Hubei University of Medicine.

Availability of data and materials
The datasets generated during and/or analysed during the current study are available from the corresponding author on reasonable request.

Declarations

Ethics approval and consent to participate
The studies involving human participants were reviewed and approved by Ethics Committee of Taihe Hospital Affiliated of Hubei University of Medicine (NO. 2024KS20), and was in accordance with the Declaration of Helsinki. Written informed consent for participation was not required for this study in accordance with the Ethics Committee of Taihe Hospital Affiliated with Hubei University of Medicine.

Competing interests
The authors declare no competing interests.

Author details
[1]Department of Nuclear Medicine, The Second Affiliated Hospital of Soochow University, Suzhou 215004, Jiangsu, China. [2]Department of Nuclear Medicine, Hubei Provincial Clinical Research Center for Precision Diagnosis and Treatment of Liver Cancer, Taihe Hospital, Hubei University of Medicine, Shiyan 442000, Hubei, China. [3]Hubei Provincial Clinical Research Center for Umbilical Cord Blood Hematopoietic Stem Cells, Taihe Hospital, Hubei University of Medicine, Shiyan 442000, Hubei, China. [4]Department of Neurological Rehabilitation Area 3, Taihe Hospital, Hubei University of Medicine, Shiyan 442000, Hubei, China. [5]Department of Radiology, Renmin Hospital of Wuhan University, Wuhan 430060, Hubei, China. [6]Department of Outpatient, Taihe Hospital, Hubei University of Medicine, Shiyan 442000, Hubei, China. [7]Department of Gastroenterology, Taihe Hospital, Hubei University of Medicine, Shiyan 442000, Hubei, China. [8]Department of Rehabilitation Medicine Center, Taihe Hospital, Hubei University of Medicine, Shiyan 442000, Hubei, China.

Received: 12 November 2024 Accepted: 31 March 2025
Published online: 09 May 2025

References

1. Sung H, et al. Global cancer statistics 2020: GLOBOCAN estimates of incidence and mortality worldwide for 36 cancers in 185 countries. CA Cancer J Clin. 2021;71:209–49.
2. Morgan E, et al. The global landscape of esophageal squamous cell carcinoma and esophageal adenocarcinoma incidence and mortality

in 2020 and projections to 2040: new estimates from GLOBOCAN 2020. Gastroenterology. 2022;163:649-658.e2.
3. Siegel RL, Giaquinto AN, Jemal A. Cancer statistics, 2024. CA Cancer J Clin. 2024;74:12–49.
4. Zheng R, et al. Cancer incidence and mortality in China, 2016. J Natl Cancer Cent. 2022;2:1–9.
5. Yang Y-M, Hong P, Xu WW, He Q-Y, Li B. Advances in targeted therapy for esophageal cancer. Signal Transduct Targeted Ther. 2020;5:229.
6. Ohashi S, et al. Recent advances from basic and clinical studies of esophageal squamous cell carcinoma. Gastroenterology. 2015;149:1700–15.
7. Toh Y, et al. Alcohol drinking, cigarette smoking, and the development of squamous cell carcinoma of the esophagus: molecular mechanisms of carcinogenesis. Int J Clin Oncol. 2010;15:135–44.
8. Helderman NC, et al. Molecular functions of MCM8 and MCM9 and their associated pathologies. iScience. 2023;26:106737.
9. Li Z, Xu X. Post-translational modifications of the mini-chromosome maintenance proteins in DNA replication. Genes. 2019;10:331.
10. Griffin WC, Trakselis MA. The MCM8/9 complex: a recent recruit to the roster of helicases involved in genome maintenance. DNA Repair. 2019;76:1–10.
11. Teng C, et al. The roles of RNA N6-methyladenosine in esophageal cancer. Heliyon. 2022;8: e11430.
12. Meng W, Han Y, Li B, Li H. The diverse role of RNA methylation in esophageal cancer. ABBS. 2023;55:988–1000.
13. Hong L, et al. Angiogenesis-related molecular targets in esophageal cancer. Expert Opin Invest Drugs. 2011;20:637–44.
14. Barzi A, Lenz H-J. Angiogenesis-related agents in esophageal cancer. Expert Opin Biol Ther. 2012;12:1335–45.
15. Yu S, et al. Function and mechanism of MCM8 in the development and progression of colorectal cancer. J Transl Med. 2023;21:623.
16. Liu X-S, et al. Expression patterns of MCM8 in lung adenocarcinoma and its correlation with key biological processes. Eur J Med Res. 2025;30:149.
17. Morii I, et al. Inhibiting the MCM8-9 complex selectively sensitizes cancer cells to cisplatin and olaparib. Cancer Sci. 2019;110:1044–53.
18. Tomczak K, Czerwińska P, Wiznerowicz M. Review the Cancer Genome Atlas (TCGA): an immeasurable source of knowledge. Współczesna Onkol. 2015;1A:68–77.
19. Barrett T, et al. NCBI GEO: archive for functional genomics data sets—update. Nucleic Acids Res. 2012;41:D991–5.
20. Love MI, Huber W, Anders S. Moderated estimation of fold change and dispersion for RNA-seq data with DESeq2. Genome Biol. 2014;15:550.
21. Ritchie ME, et al. limma powers differential expression analyses for RNA-sequencing and microarray studies. Nucleic Acids Res. 2015;43: e47.
22. Liu J, et al. An integrated TCGA pan-cancer clinical data resource to drive high-quality survival outcome analytics. Cell. 2018;173:400-416.e11.
23. Conway JR, Lex A, Gehlenborg N. UpSetR: an R package for the visualization of intersecting sets and their properties. Method Biochem Anal. 2017;33:2938–40.
24. Wickham H. Data analysis. In: Wickham H, editor. Ggplot2: Elegant graphics for data analysis. Cham: Springer International Publishing; 2016. pp. 189–201. https://doi.org/10.1007/978-3-319-24277-4_9.
25. Dai M, et al. Cholesterol synthetase DHCR24 induced by insulin aggravates cancer invasion and progesterone resistance in endometrial carcinoma. Sci Rep. 2017;7:41404.
26. Liu X-S, et al. Pan-cancer analysis reveals correlation between RAB3B expression and tumor heterogeneity, immune microenvironment, and prognosis in multiple cancers. Sci Rep. 2024;14:9881.
27. Zeileis A, Hornik K, Murrell P. Escaping RGBland: selecting colors for statistical graphics. Comput Stat Data Anal. 2009;53:3259–70.
28. Yu G, Wang L-G, Han Y, He Q-Y. clusterProfiler: an R package for comparing biological themes among gene clusters. OMICS: J Integr Biol. 2012;16:284–7.
29. Tang Z, et al. GEPIA: a web server for cancer and normal gene expression profiling and interactive analyses. Nucleic Acids Res. 2017;45:W98–102.
30. Li Y, et al. Molecular characterization and clinical relevance of m6A regulators across 33 cancer types. Mol Cancer. 2019;18:137–137.
31. Qing X, et al. Molecular characteristics, clinical significance, and cancer immune interactions of angiogenesis-associated genes in gastric cancer. Front Immunol. 2022;13: 843077.
32. Paraskevopoulou MD, et al. DIANA-microT web server v5.0: service integration into miRNA functional analysis workflows. Nucleic Acids Res. 2013;41:W169–73.
33. Li JH, Liu S, Zhou H, Qu LH, Yang JH. starBase v2. 0: decoding miRNA-ceRNA, miRNA-ncRNA and protein–RNA interaction networks from large-scale CLIP-Seq data. Nucleic Acids Res. 2014;42(D1):D92–7.
34. Chang L, Zhou G, Soufan O, Xia J. miRNet 2.0: network-based visual analytics for miRNA functional analysis and systems biology. Nucleic Acids Res. 2020;48(W1):W244–51.
35. Rehmsmeier M, Steffen P, Höchsmann M, Giegerich R. Fast and effective prediction of microRNA/target duplexes. RNA. 2004;10:1507–17.
36. Chen X, Zhang Y, He J, Li Y. Identification of STAT5B as a biomarker for an early diagnosis of endometrial carcinoma. Biocell. 2023;47:2283–300.
37. Sun H, et al. Increased MAD2L2 expression predicts poor clinical outcome in Colon Adenocarcinoma. Biocell. 2023;47:607–18.
38. Qiu J, Fu Z, Wen H, Chen Y. Identification of the novel prognostic biomarker SERPINH1 reveals its relationship with immunology in gastric cancer. Oncologie. 2023;0:367–79.
39. Wu Z, et al. A multi-cancer analysis unveils ITGBL1 as a cancer prognostic molecule and a novel immunotherapy target. Oncologie. 2024;26:195–210.
40. Chen S, et al. XRCC1, ABCB1, CYP3A5 and GSTP1 gene polymorphism associated with platinum-based drugs induced hematotoxicity in Chinese oesophageal cancer patients. Med Adv. 2023;1:133–45.
41. He F, et al. Esophageal cancer: trends in incidence and mortality in China from 2005 to 2015. Cancer Med. 2021;10:1839–47.
42. Liu X-S, et al. METTL3 as a novel diagnosis and treatment biomarker and its association with glycolysis, cuproptosis and ceRNA in oesophageal carcinoma. J Cell Mol Med. 2024;28: e18195.
43. Liu X-S, et al. Functional enrichment analysis reveals the involvement of DARS2 in multiple biological pathways and its potential as a therapeutic target in esophageal carcinoma. Aging-us. 2024;16:3934–54.
44. Liu X-S, et al. TRIP6 a potential diagnostic marker for colorectal cancer with glycolysis and immune infiltration association. Sci Rep. 2024;14:4042.
45. Wu B, Xi S. Bioinformatics analysis of the transcriptional expression of minichromosome maintenance proteins as potential indicators of survival in patients with cervical cancer. BMC Cancer. 2021;21:928.
46. Yu M, Wang H, Xu H, Lv Y, Li Q. High MCM8 expression correlates with unfavorable prognosis and induces immune cell infiltration in hepatocellular carcinoma. Aging. 2022;14:10027–49.
47. Peng Y-P, et al. The expression and prognostic roles of MCMs in pancreatic cancer. PLoS ONE. 2016;11: e0164150.
48. Guan Y, Ma J, Song W. Identification of circRNA–miRNA–mRNA regulatory network in gastric cancer by analysis of microarray data. Cancer Cell Int. 2019;19:183.
49. Zhu W, et al. Knockdown of MCM8 inhibits development and progression of bladder cancer in vitro and in vivo. Cancer Cell Int. 2021;21:242.
50. Macheret M, Halazonetis TD. DNA replication stress as a hallmark of cancer. Annu Rev Pathol. 2015;10:425–48.
51. Yuen KWY, Montpetit B, Hieter P. The kinetochore and cancer: what's the connection? Curr Opin Cell Biol. 2005;17:576–82.
52. Peake JD, Noguchi E. Fanconi anemia: current insights regarding epidemiology, cancer, and DNA repair. Hum Genet. 2022;141:1811–36.
53. Guo H, et al. m6A reader HNRNPA2B1 promotes esophageal cancer progression via up-regulation of ACLY and ACC1. Front Oncol. 2020;10: 553045.
54. Liu X-S, et al. Comprehensive Analysis of YTHDF1 Immune Infiltrates and ceRNA in Human Esophageal Carcinoma. Front Genet. 2022;13: 835265.
55. Chen S, et al. Competing endogenous RNA network for esophageal cancer progression. Ann Transl Med. 2021;9:1473–1473.
56. Ma Z, et al. E2F1 reduces Sorafenib's sensitivity of esophageal carcinoma cells via modulating the miR-29c-3p/COL11A1 signaling axis. CMP. 2023;17:36876834.
57. Hu L, Cao H, Zheng L, Li R. BBOX1-AS1 activates hedgehog signaling pathway to facilitate the proliferation and stemness of esophageal squamous cell carcinoma cells via miR-506-5p/EIF5A/PTCH1 Axis. CMP. 2023;16:894–904.
58. Wang M, et al. Long non-coding RNA RP11–197K6.1 as ceRNA promotes colorectal cancer progression via miR-135a-5p/DLX5 axis. J Transl Med. 2024;22:469.

59. Berhane T, et al. Knockdown of the long noncoding RNA PURPL induces apoptosis and sensitizes liver cancer cells to doxorubicin. Sci Rep. 2022;12:19502.

Publisher's Note